Acquisition and Analysis of Cryogenic Transmission Electron Microscope Biological Images

Lewis Collier
URI CSC592
Final Report
Spring 2005

This technical memorandum describes the project "Acquisition and Analysis of Cryogenic Transmission Electron Microscope Biological Images", which was performed during the URI CSC592 Bio-Informatics class during the spring semester 2005.

Abstract – Methods of determining the geometric shape and size of LDL macromolecules were investigated. The methods consisted of application of computer vision techniques to cryogenic transmission electron microscope images. Direct correlation of computer-generated geometric models was investigated to determine the limits of accuracy that can be expected from the method, given the expected discoid shape of the LDL. The processing shows that the discoid shape can be verified using small angle rotations that are more amenable to the limitations of CTEM.

1 INTRODUCTION

This section provides an introduction to the project. In addition, team members are acknowledged and references are listed.

1.1 Biological Impetus

The biologic target of interest is lipoprotein. Lipoproteins are a combination of lipid (fat) and proteins. Together, they make a macromolecule that acts as a suitcase for ferrying cholesterol throughout the human body. High-density lipoproteins (HDL) are generally smaller (than HDL) with more protein than fat. HDL acts as a carrier of cholesterol from the body back to the liver for processing. Low-density lipoproteins (LDL) are generally larger (than HDL) with more fat than protein. LDL acts as a carrier of cholesterol from the liver to the cells in the body.

The size of LDL packages is important to the understanding of heart disease. The smaller LDL packages are considered to be a leading cause of arterial plague that can lead to heart attacks. In general, small numbers of bigger LDL particles is tied to better health while larger numbers of smaller LDL particles correlates to worse health. A better method of quantifying the shape and size of various LDL particles will allow for a better understanding of the biological mechanisms in this area.

The research performed in this project is important because size differences in HDL and LDL have been shown to be very important in medical studies. In a study of diabetics [Vakk2003], changes in LDL size accounted for part of the antiatherogenic effect of type-2 diabetes. In this study, increases of only 0.98nm in LDL diameter showed a detectable change. And even though conventional wisdom states that HDL is "good" cholesterol, another study [Otvo1998] showed that high concentrations of small HDL resulted in a 15-fold increase in the risk of heart disease. A method of determining the actual size and shape of lipoproteins is needed to allow for further modeling and analysis.

1.2 Team

Even though I was the only student from this class working on this project, there were several people who assisted me and provided welcome efforts on this project. I would like to take this opportunity to acknowledge and thank them for their efforts.

Dr. Lenore Martin, Associate Professor, URI Department of Cell and Molecular Biology, martin@mail.uri.edu. Dr. Martin suggested this project and has provided much assistance in understanding the biology and the importance of this work.

Dr. Joan Peckham, Professor, URI Department of Computer Science, joan@cs.uri.edu, Dr. Peckham provided encouragement to me to take this class and during the project.

Dr. Jean-Yves Herve', Assistant Professor, URI Department of Computer Science, herve@cs.uri.edu. Dr. Herve' provided many good ideas regarding the image processing techniques to be used and helped direct the geometric modeling of discoids with Maya. He also provided the base CSC583 library classes, which provided a basis for the code that was written for this project.

Dr. Arijit Bose, Professor and Chair, URI Department of Chemical Engineering, bosea@egr.uri.edu. Dr. Bose provided significant insights into the CTEM process.

Mr. Paul Johnson, Manager, URI Electron Microscopy and Imaging Facility, pwj419@mail.uri.edu. Mr. Johnson provided help with understanding the JEOL-1200EX TEM and its capabilities.

Mr. Matt Kayala, Student, URI Department of Computer Science, matt.Kayala@gmail.com, Mr. Kayala performed modeling of discoid shapes with Maya to generate template images for processing studies.

PFAST Team, CSC592 Project Team, The PFAST project team provided many helpful comments during their in-class reviews during the semester.

1.3 References

[Antw1994] Rik van Antwerpen and John C. Gilkey, “Cryo-electron microscopy reveals human low density lipoprotein substructure”, Journal of Lipid Research Volume 35, 1994 pp:2223-2231.

[Antw1997] Rik van Antwerpen, G. Chi Chen, R. Pullinger, John P. Kane, Michael LaBelle, Ronald M. Krauss, Cesar Luna-Chavez, Trudy M. Forte, and John C. Gilkey, “Cryo-electron microscopy of low density lipoprotein and reconstituted discoidal high density lipoprotein: imaging of the apolipoprotein moiety”, Journal of Lipid Research Volume 38, 1997 pp:659-669.

[Antw1999] Rik van Antwerpen, Michael La Belle, Edita Navratilova, and Ronald M. Krauss, “Structural hetrogenity of apoB-containing lipoproteins visualized using cryo-electron microscopy”, Journal of Lipid Research Volume 40, 1999 pp:1827-1836.

[Mara1996] http://www.cnb.uam.es/~bioinfo/Software/xmipp/xmippwww.html

[Gata2001] http://www.gatan.com/imaging/tem_auto.html

[Otvo1998] James Otvos, R. Marabini, I.M. Masegosa, M.C. San Martín, S. Marco, J. J. Fernández, L. G. de la Fraga, C. Vaquerizo, and J.M. Carazo, “Radio Signals Give New Spectrum For Cholesterol Lipoprotein Readings”, Arteriosclerosis, Thrombosis and Vascular Biology: Journal of the American Heart Association, NR 98-4910

[Teer2004] Tom Teerlink, Peter G. Scheffer, Stephan J. L. Bakker, and Robert J. Heine, “Combined data from LDL composition and size measurement are compatible with a discoid particle shape”, Journal of Lipid Research Volume 45, 2004 pp:954-966.

[USCD2004] http://em-outreach.ucsd.edu/index.html

[Vakk2003] Juha Vakkilainen, MD; George Steiner, MD; Jean-Claude Ansquer, MD; Francois Aubin, MD; Stephanie Rattier, MSc; Christelle Foucher, PhD; Anders Hamsten, MD; Marja-Riitta Taskinen, MD; “Relationships Between Low-Density Lipoprotein Particle Size, Plasma Lipoproteins, and Progression of Coronary Artery Disease : The Diabetes Atherosclerosis Intervention Study (DAIS)”, Circulation (www.circulationaha.org), DOI: 10.1161/01.CIR.0000057982.50167.6E

2 BACKGROUND INFORMATION

This section provides background information regarding the project. This background includes an overview of previous research, an introduction to transmission electron microscopy, and existing CTEM processing.

2.1 Previous Research

This project was directed towards determining the shape and size of lipoprotein macromolecules. Specifically, prior research has concluded that LDL macromolecules are discoid in shape, as opposed to the previously held theory that they were spheres. This research, however, did not apply computer vision to help establish the discoid shape and size. In one set of studies [Antw94, Antw97, Antw99] sub-optimal methods were used to measure the LDL shapes from cryogenic transmission electron microscope (CTEM) images. More recent studies [Teer04] used volume/mass ratios of high performance gel chromatography (HPGC) to determine the shape. This study matched data based on a geometric model of a disc with varying height rather than directly from images of the macromolecules.

In the 1994 research by Antwerpen, et. al. [Antw1994], CTEM images were examined at rotations of –45, 0, and +45 degrees. From these images (see Figure 1) candidate objects were considered. The numbered objects are 3-tuples, which represent a discoid rotated at the orientations of –45, 0, and +45 degrees. Object 3 corresponds to the simulated discs in Figure 2.This study measured the diameter and height of the discs but did not present a thickness of the wall as seen in the projection at 0 degrees.

Additional efforts by this research group [Antw1997, Antw1999] extended their previous results to indicate that LDL was actually divided into classes based on size. Again, simple projections at –45, 0, and +45 degrees were used to measure the dimensions. These measurements were done using Adobe Photoshop tools on scanned images of photographs from the CTEM equipment. These studies, however, did show a more clearly defined image as is shown in Figure 3.

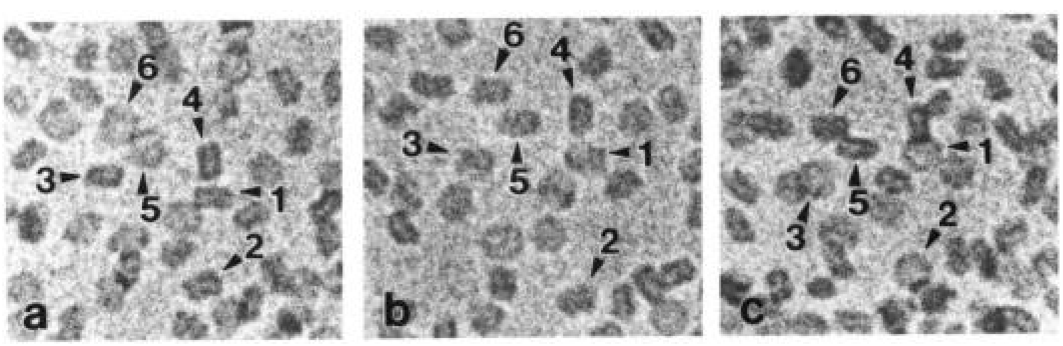

Figure 1. Antwerpen Images From 1994

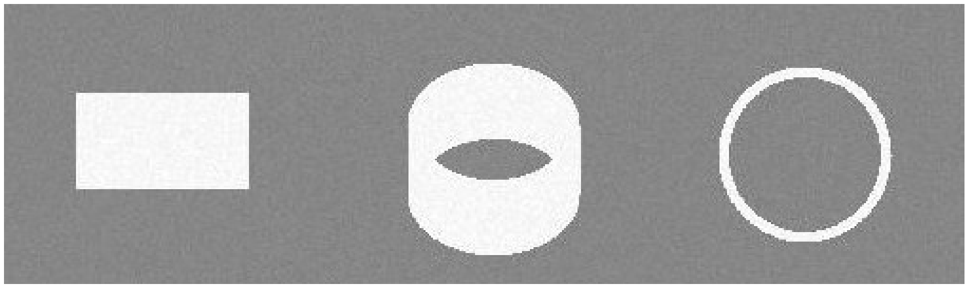

Figure 2. Simulated Discs

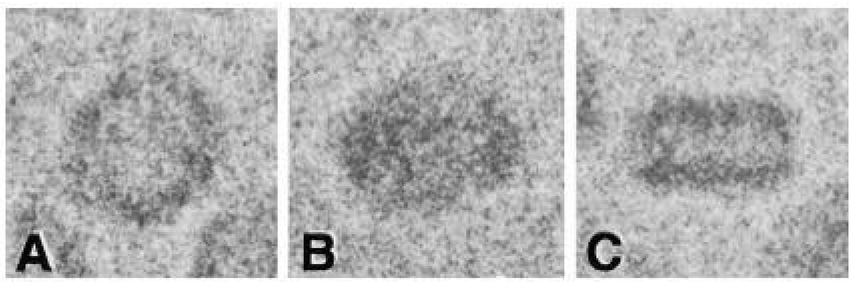

Figure 3. Antwerpen Images From 1999

2.2 Introduction to TEM

A significant component of this research involves understanding the nature of the imaging equipment to be used. Since the CTEM process images frozen samples, long or high dose exposures can lead to sample degradation. Steps must be taken to ensure that the best possible images are obtained so that the samples are not destroyed during the CTEM imaging.

A basic understanding of the TEM imaging can be gleaned from current CRT TV tubes. In CRT tubes, the back of the tube, the electron gun, produces a stream of electrons that is directed to the screen. Here, the electrons strike regions of phosphors to create illumination from the front of the TV screen.

In a TEM, the same basic principle is employed. However, the stream of electrons is larger in area and this area can be adjusted. In a TV, the goal is to strike a single pixel as the beam is scanned along the rows and columns of the screen. In a TEM, the goal is to provide a constant flow of electrons at a steady density. In the TV, the goal of the e-beam is to strike the phosphors to create illumination. In the TEM, the e-beam is passed through the sample in order to scatter some of the electrons. Thus, darker regions indicate more dense regions of the sample. As with the TV, the electrons are then directed to strike a medium that will allow for the image to be viewed. In our case, the medium is a scintillator that also creates photons. These photons are then measured with a charge-coupled device (CCD) camera.

The e-beam can change the characteristics of the observed image. As one can imaging, a beam that is too wide in a TV will result in a muddied image. Too many pixels will be illuminated when only a single pixel should be illuminated by the e-beam. Likewise, in TEM, the same holds true. However, the beam width is adjustable so that the magnification and focus can be adjusted to improve the clarity of the image.

There are many adjustments that can be made and the actual adjustments will vary from model to model. A detailed description of these factors is provided in [USCD2004]. Of importance to this project is that fact that these settings can influence the final image. As with standard photography, changes in zoom and aperture can result in a perfect picture of a blurry mess. Since our goal is to apply computer vision techniques to the images, it only makes sense to consider these settings when acquiring the images.

2.3 Existing CTEM Processing

While there is a plethora of image processing software and applications, there is a dearth of processing directed towards CTEM images. Given the previously mentioned list of issues that must be addressed regarding the setup of the TEM equipment, there is ample opportunity for both setup and processing of CTEM imagery. A fairly exhaustive search, however, reveals only a handful of similar items.

A leader in this field is the “Baker” research group at USCD. Besides the introduction to TEM [USCD2004], they also list several programs that can be used for TEM image processing. Most of this software, however, is geared towards to 3-D reconstruction of viruses from multiple images. Since the viruses are the same size in all samples, his technique is to acquire many images and create projection slices. From these slices, he can build 3-D models. This technique, however, will not work for LDL particles since the sizes vary in the different classes of LDL.

There is some “auto tuning” software from Gatan [Gata2001] that was found but this software only works with a Gatan brand camera (URI has JEOL) and it has its own PCI-based hardware for processing.

Another software package is Xmipp [Mara1996] but again, this is used for 3-D reconstruction from slices.

3 Project Plan

This project will provide assistance to the two above mentioned image acquisition problems as well as provide computer vision assistance with the image analysis.

3.1 Image Acquisition Support Software

The continuous exposure will be addressed by using computer vision to analyze the images rather than requiring human vision. Since only single exposures are required for computer vision, the TEM beam can be blanked or "turned off" while the prior image is analyzed. Once an ROI and reference points within the ROI are defined, the computer can provide the required stage movements and TEM settings required to achieve focus or centering of the reference items. Once the manual stage has been repositioned, a new image can then be acquired for analysis, thus creating a feedback loop that does not require continuous exposure of the sample.

The support software will also provide assistance for setting the TEM parameters for adjustment of metrics such as background processing, focus, and contrast. An understanding of the bright and dark state of the TEM and its CCD is the first step in processing. Outlier pixels can be detected so that the final image can be corrected for these CCD defects. In addition, the dark and bright state images can be saved for down-stream processing. For example, since an FFT will be used for faster correlation processing, the FFT of the background can be analyzed to see if there are any spatially dependent components of the noise background. Removal of these can help the final image processing.

Once the background state is known, the TEM settings (such as e-beam energy, and density) can be adjusted with a sample in place to help maximize the detail of the image. Higher energy electrons produce sharper images (since they pass through the sample with less attenuation and deflection) but they can also lead to melting. A balance between the two extremes is needed to get the best images. Other parameters (e.g. exposure time) can also be adjusted to assist in the image detail. These parameters will be studied to help increase the resolution of the acquired images.

3.2 Image Processing Analysis Software

The multiple perspective angles will be addressed by applying geometry and computer vision to the manual stages. Once a perspective has been identified, a next location can be determined and the required manual stage movements can be provided to the human operator. Once the operator has performed this movement, a new image can be acquired and analyzed. This fine-tuning process can be repeated as necessary in order to get a well-defined image at each perspective angle. If sufficient images can be acquired, a movie of the rotation of a lipid of interest can be generated.

The ultimate goal of this project is to allow for multiple images to be acquired and analyzed to provide a statistical confidence in the determined geometric parameters of the LDL. By using a high-definition model (e.g. as can be generated with Maya) the correlation of a single particle can be performed. The statistical proof, however, will come from the correlation of the same particle through a series of rotation angles. Since the previous research needed human processing, a rotation or +/- 45 degrees was needed. This led to the need for long rotate and re-focus cycles. With proper correlation, it is anticipated that small angles (maybe +/- 5 degrees) can be used to generate a series of images for correlation. If these particles are near the rotation axis then no additional refocusing is required.

3.3 Image Acquisition and Analysis

The final stage of this project is to provide image analysis of specific images in order to measure the shapes and sizes of lipids in the sample liquid. As noted above, there is some evidence that the lipids of interest are actually disks surrounded by a protein band. When viewed from the flat side, the disks appear as a dark line with a length determined from the diameter of the disk. When viewed from the top or bottom, the disks may appear invisible or they may appear as a circle. This appearance will depend upon the density of the protein belt. In any case, as the disk is rotated through perspective angles, the relative shape and darkness will change. Computer vision techniques will be applied in order to help model the expected changes in order to determine the shape of the lipid.

4 PROJECT RESULTS

This project was carried out during the spring 2005 semester as a part of the requirements for the CSC592 (Bioinformatics) coursework. The results of this project are divided into four categories: documentation, software, analysis, and setbacks.

4.1 Documentation

The documentation for this project consists of the following items:

Project Proposal – A project proposal was developed for this effort. This proposal provided the basic goals and planning for the project.

System Performance Specification (SPS) – This is a document that provides a list of the capabilities of the overall system. The SPS defines what the system shall do. It does not describe how the system shall accomplish the requirements.

For this project, a draft SPS was developed. The analysis portion of the software is fairly well describes but the image acquisition portion was not completed since access to the TEM was very limited so a detailed understanding of the capabilities of the TEM was not available.

Software Requirements Specification (SRS) – This document provides a list of the requirements of the software. The SRS describes what the software is to do and in some cases, it can also specific how to accomplish the task at hand. In addition, an SRS can contain traceability back to the SPS so that changes to the overall system performance specifications can be analyzed to determine what portions of the software will be affected. This can then be used to determine the level of effort that will be required for code alterations and retesting.

For this project, a draft SRS was developed. This SRS provides the overall design for the software for both image acquisition and analysis. The analysis portion is fairly well defined. As with the SPS, the acquisition support software design was not complete.

Final Project Report – The project documentation includes this report.

Final Presentation Slides – A final presentation on the project was also presented. The slides for this talk are included in the documentation for the project.

C++ Code – About 5,000 source lines of code (SLOC) were developed for and used in this project. This code can also be examined for more details about the processing that was performed.

4.2 Software

The software for this project consists of the following items:

4.2.1 3rd Party Software

Several pieces of software developed from other (3rd) parties was used. These software packages are:

CSC583 base classes – These are the base object classes for image processing from the CSC583 library. These classes provided the basic rendering and class definitions for image operators but with no associated image processing code. These classes were used as the basis for all processing performed in this project.

CodeWarrior v8.3 – This is the student version of CodeWarrior integrated development environment. All code was developed with options for execution on both PC and Mac platforms but all development and testing was performed on PC platforms.

GLUT v3.7.6 – This is the OpenGL Utility Toolkit as required by the CSC583 classes.

QuickTime v6.5.2 – This is the QuickTime runtime engine as required by the CSC583 classes.

OOURA 2-D FFT – This is a package of 1-D, 2-D, and 3-D FFT software from *Takuya Ooura at the Research Institute for Mathematical Sciences, Kyoto University, Kyoto 606-01 Japan.* This package was chosen because it provided a simple and easy to use coding interface that was not specific to any IDE or platform. It also provided a test suite and support for many data types and Fourier transform versions. The double precision code was copied and altered to provide a single precision version. The error of this altered single precision version was in line with expectations in the precision differences between double and dingle precision arithmetic.

4.2.2 C++ Software written by the author this semester

Approximately 5kSLOC of C++ code was developed this semester and used in this project. This code is comprised of:

General Purpose Code – Approximately 3kSLOC of general-purpose C++ image processing code was developed this semester. This code, which is located in the CodeWarrior project Collier583Lib, contains 13 modules.

The collier_VectorMath.cpp module provides a function for obtaining the vector field divergence.

The collier_ImageMath.cpp module in this library provides about 30 functions that operate on the CSC583 Raster Image class. These functions range from copies and arithmetic to statistics and thresholding.

The collier_CSC583LIB.cpp module contains basic functions and Endianosity conversion functions, which were, needed for some of the file conversion efforts.

The remaining collier_*.cpp modules provide 10 general-purpose image processing operator classes.

The two OOURA_* modules contain the code for the Ooura FFT support.

Specific Code – This is the main CTEM demonstration project. Since it was derived from a CSC583 example, all functions are in the main file (CTEM_demo.cpp) rather than in separate files. The file is divided into the following sections:

Test FFT Code – this is a function that tests the Ooura FFT code with the CSC583 raster Image data type.

Setup Functions – This code builds the disc templates, and loads in images from file.

Graphics Functions – This code sets up the basis QuickTime environment and performs basic drawing functions.

Display Functions – This code handles the display processing. There are three display functions, one for each of the windows in the demo (main, window0 and window 1).

Idle Function – This is the main function that is called when there is no user input to be handled. This function does nothing at this point other than return to the calling function.

Keyboard function – This is the function that handles keyboard input.

Mouse Functions – These functions handle mouse inputs. The mouse is used to select operations via the menus and to select X,Y positions for cursor readouts and ROI centering.

Menu Functions – These functions provide the processing when a menu command is selected. These menus handle selection of the image family to process, display of images, and drawing of titles and readouts.

Init Function – This function performs all of the initialization as required by the GLUT library for menu initialization and display management.

Main Function – This is the main function for the demonstration software. It activates the windows, assigns menus to the windows, and then uses the GLUT library for the main loop callback handling.

4.3 Analysis

The analysis portion of this project consisted of three activities. First, models of the discs were developed. Second, a study of correlation of the discs was performed to determine how well the processing could distinguish between the models. The third activity was to study how well the FFT-based correlation was able to differentiate between the models.

4.3.1 Disc Models

Two models of discs were developed in this project. The first was a simple layering of circles of varying radius and tilt angle. The second was a more complex model developed with Maya. The simple disc model parameters are shown in Figure 4. As is seen, the height (h), diameter (d), and wall thickness (t) are the pertinent parameters. The final parameter is the tilt angle. Only tilts along the horizontal axis were considered since this more closely represents the tilting of the sample on the TEM stage. These discs are constructed from a series of circles of varying radii and offsets from a center position. The middle region is completely transparent so the background is shown in this region.

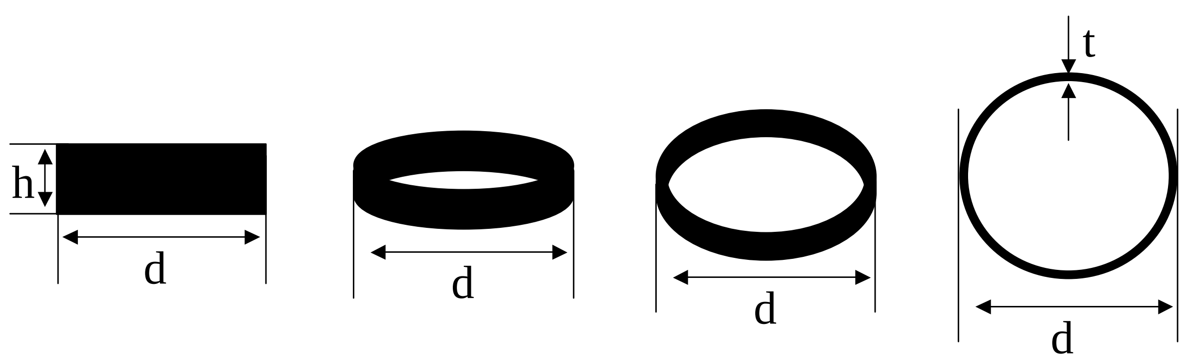

Figure 4. Simple Disc Model Parameters

The Maya program can generate a more complex model of the discs. Maya is a 3-D rendering program that is capable of translations and rotations of the models and it can include an opacity measure for the middle regions. Thus, a more complete model fo the projected image can be created so the correlation can take more of the physical features of the LDL discs into account for the correlation and projection matching. An example of some Maya discs is shown in Figure 5. This example shows a range of radii with zero degrees rotation. By rendering the image three times, once in each of the RGB color planes, a variety of pattern models can be generated.

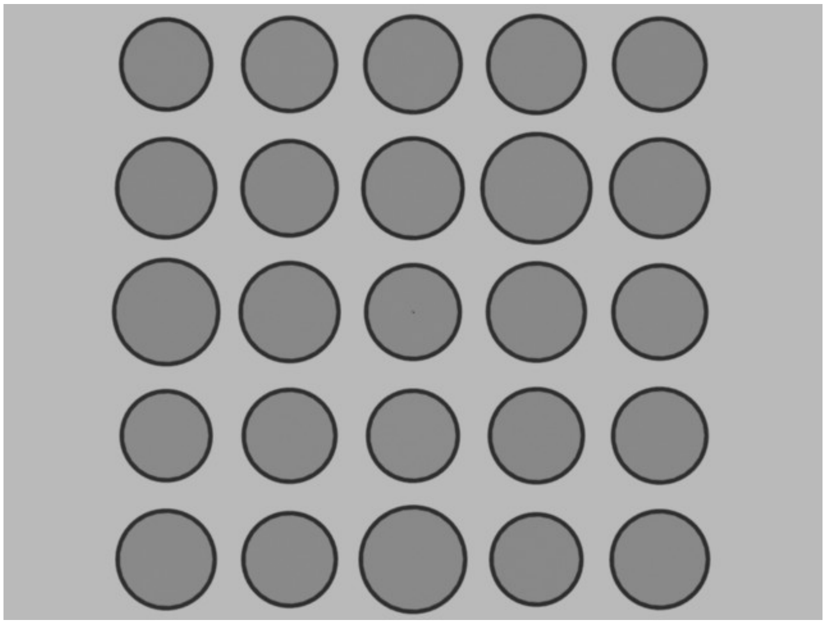

Figure 5. Maya Discs

4.3.2 Correlation Results

The first test was to see if a correlation could be applied to a decimated version of the image. This was done to decrease processing time. Since the images are expected to be 2048x2048 pixels and the templates will be on the size of 99x99 pixels, the resulting correlation will require about 42 billion floating point multiplies and adds. On a 1600 MHz P4 computer, this equates to about 825 seconds (13.75 minutes) of processing for a single image. When the image is decimated to 512x512, the requirements are reduced by a factor of 256 to approximately 3 seconds.

The results of this test are shown in Figure 6. The overall results of the correlation of a disc at a tilt angle of 45 degrees versus the same disc tilted at angles ranging from 0 to 90 degrees is shown in the left graph. The blue line shows a non-decimated correlation while the pink line shows the decimated (4:1) correlation. As is shown, the correlation function does not suffer too badly from the decimation. An expanded region around the peak is shown in the right side. Again, the decimated results suffer only slightly at the peak from the non-decimated data. Thus, the use of a decimated image can provide a good first approximation to the detection of modeled discs. And, this detection provides a processing saving of 256 over the full correlation.

The results of correlating decimated images across the range of angles (0 to 90 degrees) is shown in Figure 7. As is shown, the decimated images show a strong peak when the template tilt angle matches the base image. More importantly, the off-angle discs show a much lower correlation to the template. Again, this shows that the correlation of decimated images can be used for a first pass processing technique.

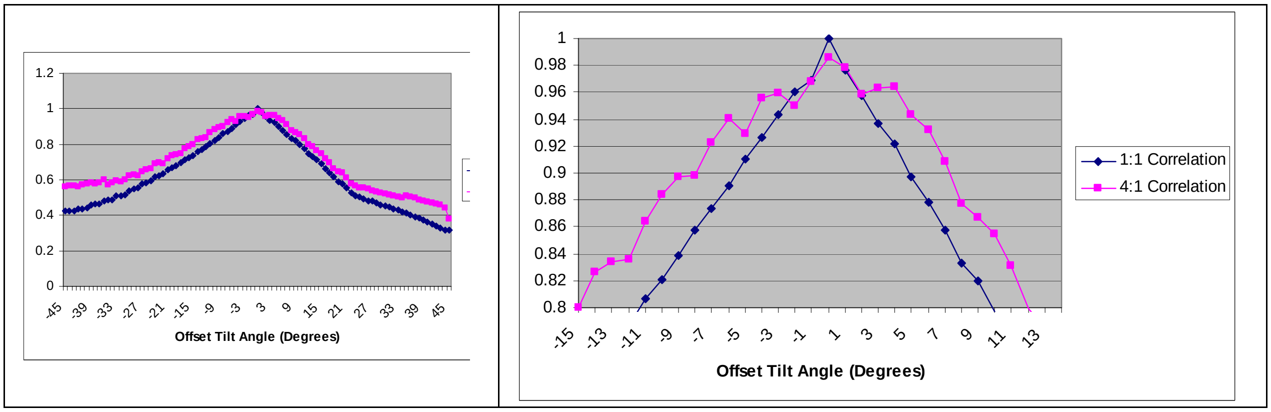

Figure 6. Decimated Correlation Results at Tilt = 45 degrees

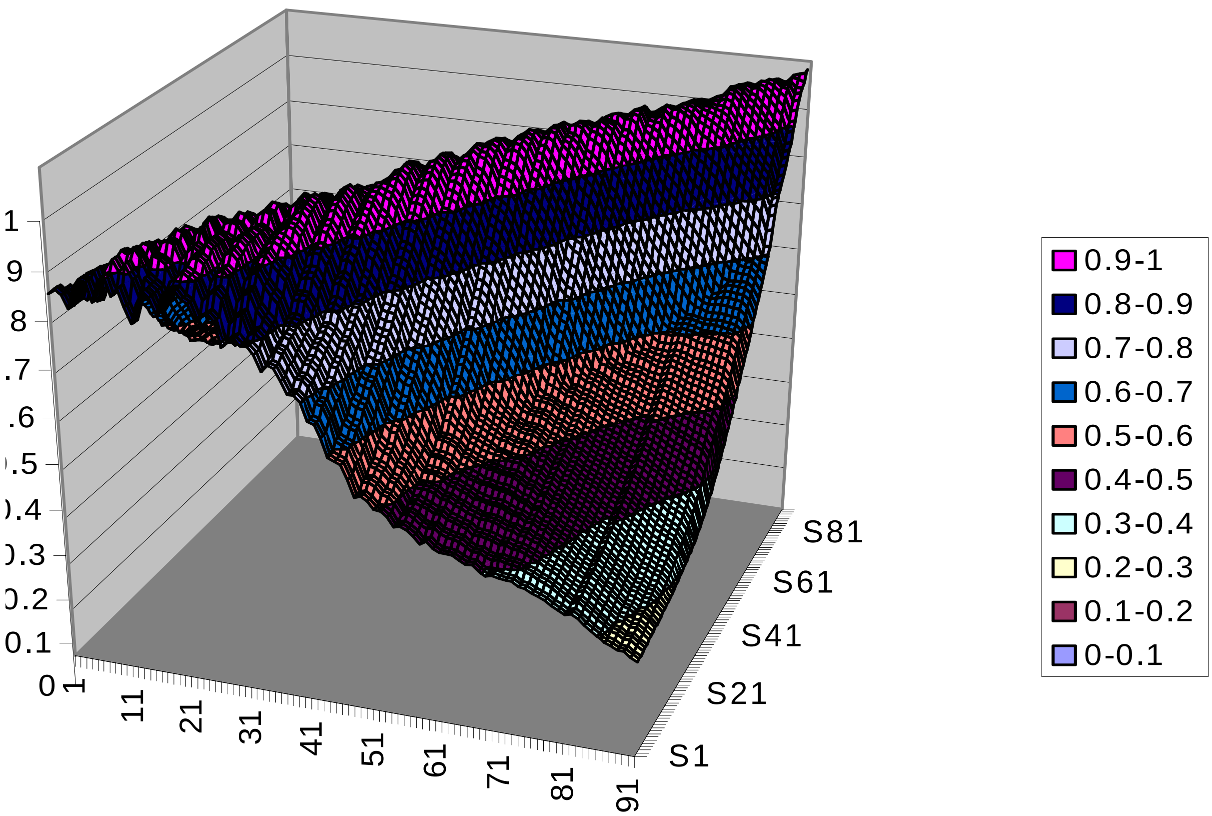

Figure 7. Decimated Correlation Results (Tilt = 0 to 90 degrees)

The next test was to correlate over ranges of radius, height, and thickness with the decimated images. These results are shown in Figure 8, Figure 9, and Figure 10. All show fairly good correlation between the varying parameter sets. This means that the decimated correlation can even be used to help distinguish between slightly varying models with differing parameters. Obviously a final match needs to be made with a more robust technique but this processing can allow for real-time feedback.

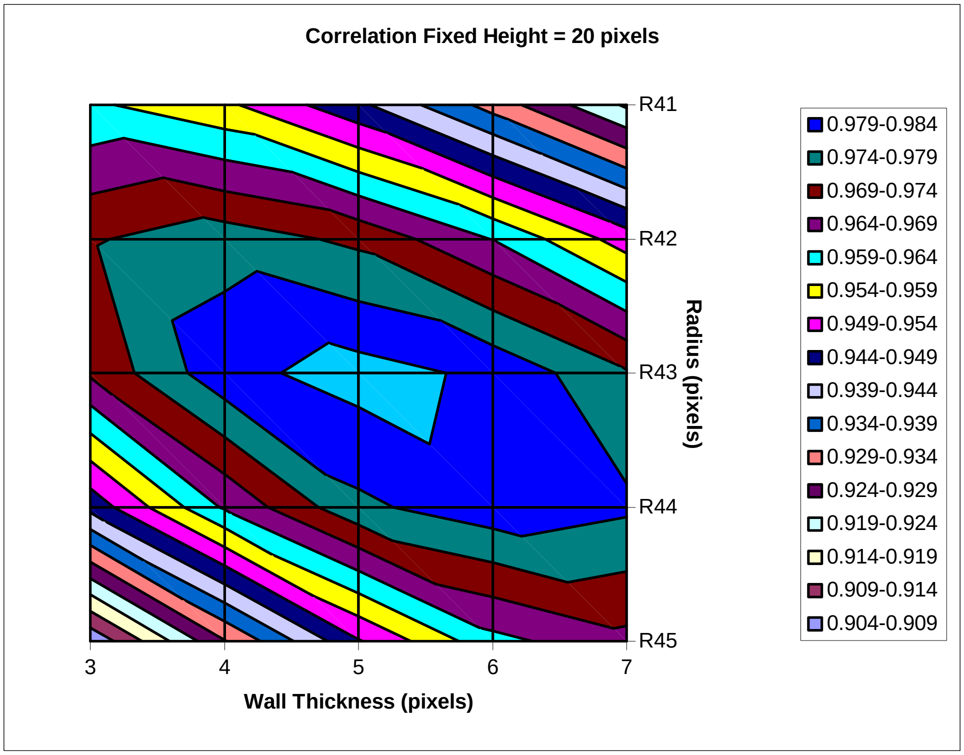

Figure 8. Decimated Correlation (H=20; R=41-45; T=3-7)

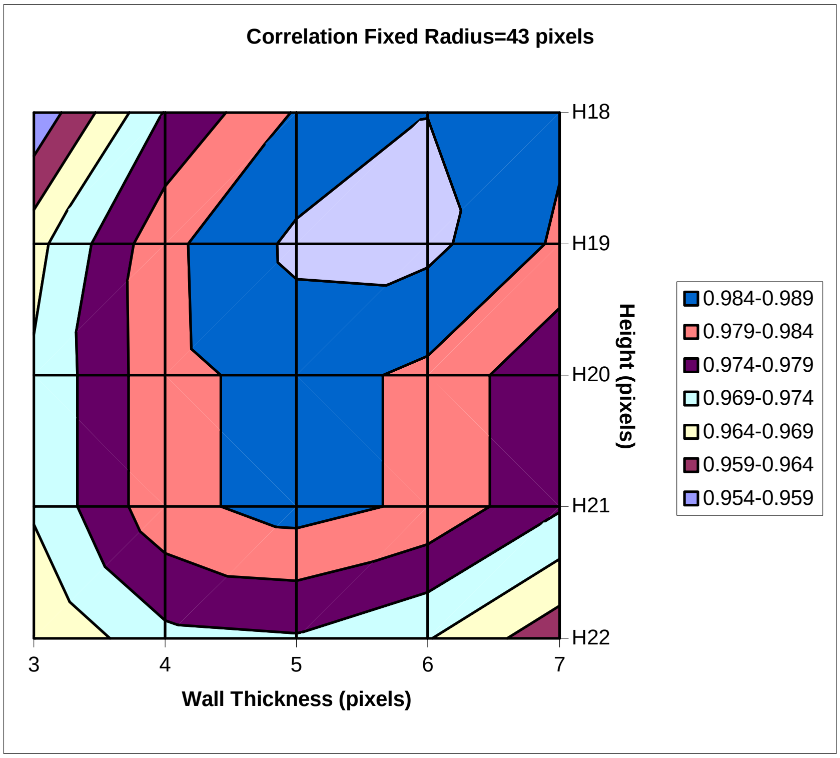

Figure 9. Decimated Correlation (H=20; R=41-45; T=3-7)

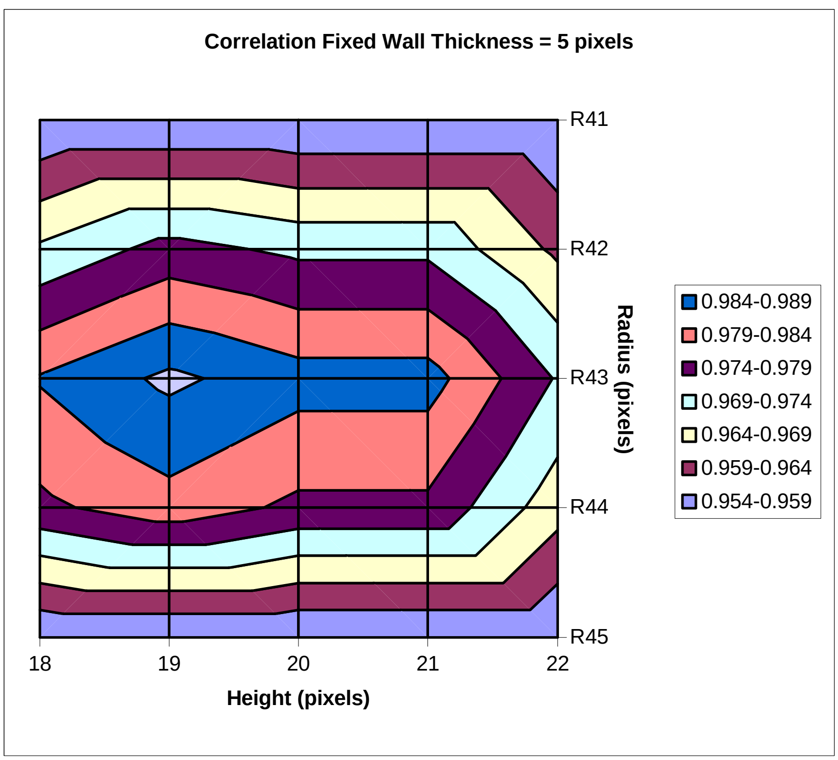

Figure 10. Decimated Correlation (T=5; R=41-45; H=18-22)

4.3.3 Correlation via FFT Results

Use of the FFT/multiply/IFFT leads to significantly faster processing. The entire processing is on the order of 2 seconds for the entire image. This is better than the 3 seconds for the decimated image but in theory, the processing matches the full correlation which takes 825 seconds.

The same tests were run with the code using FFT, multiply, and IFFT for the effective correlation processing. This run covered R=37 to 49, T=1 to 9, and H=15 to 25. With the faster FFT processing, these 1287 tests took approximately 55 hours on the P4-1.6Ghz CPU. Unfortunately, the post-analysis software did not examine a large enough area to measure the peak values. The FFT correlation, as implemented, resulted in a shift of approximately 10 to 15 pixels from the expected location so the peak values were not found.

The cause for the shift needs to be studied further. The shift is only in the Y direction so it may be an artifact of the order of applying the FFTs or it may be an artifact of the tilt angle of the discs. In either case, the cause and effect on the results needs to be studied more.

4.4 Setbacks

As in any project, this project has some issues that resulted in setbacks to the scope of the final results. The major issue was lack of access to the TEM equipment. Since the process of image acquisition could not be performed, none of the detailed design for the acquisition support software could be completed. In addition, no new images of LDL samples could be obtained. These setbacks affected the project in the following ways:

Design and Documentation – The SPS and SRS are not as complete as was hoped since the details of the acquisition support could not be analyzed.

Software – Since there were no new images to test the analysis as planed, models of the discs had to be created. The simple models worked sufficiently well to test the basic processing (as described above) but the Maya models required significant effort (both in the development of the Maya generation and in file conversion to read the files into the SCS583 framework).

Analysis – Since there was no design or development of the acquisition support software, this portion of the analysis could not be performed. Since there were no new images, the goal of testing the analysis software on real images could not be performed. This included the goal of matching discs from small rotation angles. Finally, the previous images had been saved in 8 bit format instead of the desired 12 bit images so the dynamics of the CCD and TEM images could not be studied.

5 SUMMARY

Despite the setbacks, this project has provided a good starting point for further studies of CTEM images of LDL.

5.1 Future Work

Future efforts are directed towards the analysis and software. As noted above, additional work needs to be performed on the analysis to determine the cause of the shift in the FFT results. And, even with the speed of FFTs, faster matching algorithms would be desirable, as larger format CCD cameras will result in higher resolution images that will take too long to analyze. The software needs to be fine tuned for faster operation and the acquisition support software needs to be designed and developed.

The immediate goal is to get funding complete the software and do a complete analysis of shapes and sizes of VLDL, IDL, LDL, and maybe even HDL.

5.2 Conclusions

CTEM has been previously used to measure LDL particles but these studies were not able to provide conclusive evidence of the shape and size parameters. A lack of analysis capabilities has hindered these previous studies.

This project has laid the foundation for completing a study of LDL and HDL particles. The requirements and design for computer vision software to aid in acquisition and analysis of lipoprotein CTEM images was begun. Analysis software has been developed to provide correlation of projected (2-D) images of 3-D objects. This software has been used to analyze artificially generated discoid objects to determine the analysis limits of the method. The results of this project have shown that the proposed method can be used to determine the shape and size of LDL particles to a very high degree of accuracy.

6 PROTOTYPE DEMONSTRATION ANALYSIS SOFTWARE

This section provides information regarding the prototype demonstration analysis software. The executable file is named “CTEM_demo – static.EXE”. As a part of the CSC583 directory structure, this executable expects to reside in a directory named “C:\SDKs\CSC583Lib\SDK\Demos\C++\CTEM_DEMO”. The executable file is a MS-DOS console application that utilizes GLUT and QuickTime for graphics outputs. Please refer to the installation notes with the software for information about how to install the CodeWarrior, GLUT, and QT.

The CTEM_Demo software consists of a main window and two display regions. This screen is shown in Figure 11. The main window (which includes the black background area) has a menu to set the background color and to select the family of images to be processed. The left window is a decimated (4:1) version of the current 2Kx2K image. The right window is a 1:1 representation of the area as denoted by the red ROI boundary. There is also a MS-DOS window (not shown) that is used for diagnostic messages (e.g. timing information).

6.1 Main Window

The main window has a menu with 6 items. These items, which are accessed via the right mouse button, are:

- Quit – exits the program. The MS-DOS window may need to receive a <CR> to close.
- Reset Images – causes the images to be reset to the initial state. This is used in case processing has changed images and it is desired to restore them.
- Process Analysis Image – causes the internal memory to use the self-generated analysis image (shown in Figure 11) for all processing.
- Process Maya Image – causes the internal memory to use an image that was generated by Maya for all processing. While functional, this code is currently set up to use a copy of the analysis images. A compile time option can be changed to read in the Maya images once they are ready for use.
- Process Blood Image – causes the internal memory to use a previously captured image of blood. This image does not match the expected statistics or magnification but is provided for demonstration purposes.
- Color – leads to a sub-menu to set the background color. A setting other than black may be desired since some of the processing can lead to a black image.

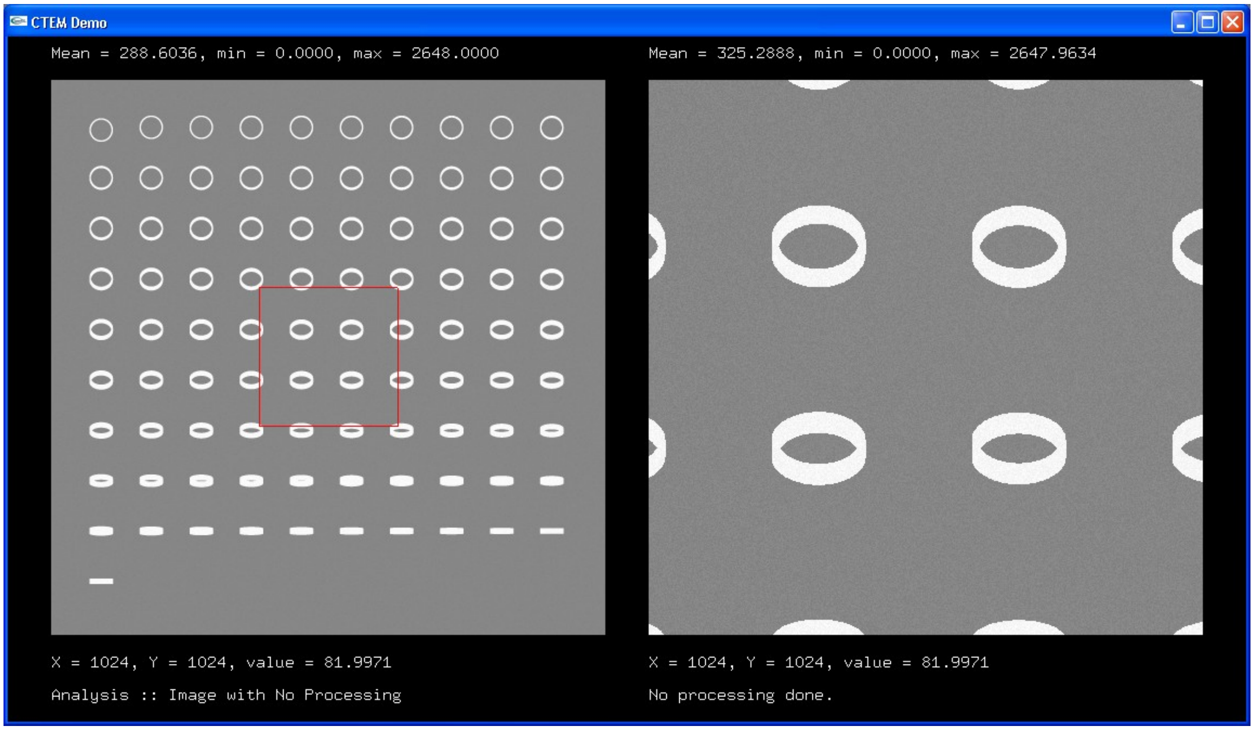

Figure 11. Demonstration Software Main Screen

The main window also provides 6 readout items. These items are:

- Left hand window statistics – which are presented above the left hand window.
- Right hand window statistics – which are presented above the right hand window.
- Left hand window cursor readout – which is presented immediately below the left window.
- Right hand window cursor readout – which is presented immediately below the right window.
- Family and processing status – which is presented below the left window. This denotes the current family of images being processed as well which of the images is being displayed.
- Processing complete status – which is presented below the right window. This denotes what processing was last applied to the currently displayed results.

6.2 Left Window

The left window shows the currently selected image. The image, which is 2Kx2K in size, is shown as decimated to fit in the 512x512 space. The 12-bit data is converted to a floating point representation. Since averaging is used to decimate the data, the statistics may not match exactly between the two windows. The cursor readout and ROI center can be changed by pressing the left mouse button. The right mouse button provides access to the 9 menu options.

- Quit – exits the program. The MS-DOS window may need to receive a <CR> to close.
- Reset Images – causes the images to be reset to the initial state. This is used in case processing has changed images and it is desired to restore them.
- Toggle show Max Point – causes a red crosshair to be displayed at the location with the maximum value.
- Show Base Image – displays the decimated version of the base image for the current family. This is the image with no processing applied.
- Show FFT of Base Image – displays the decimated version of the FFT of the base image.
- Show Template Image – displays the decimated version of the template image. This is the image that is used for the FFT correlation processing. This image is split so that it is centered at a virtual 0,0 point. A similar image that is not split, which cannot be viewed, is used for the correlation processing.
- Show FFT of Template Image – displays the decimated version of the FFT of the template image.
- Show Results Image – displays the most recent results. The results are based upon the processing that has been selected in the right hand window.
- Show FFT of Results Image –displays the decimated version of the FFT of the current results image.

For the analysis case, the base image is a series of discs at tilt angles ranging from 0 to 90 degrees. The disc in the upper left corner is the disc at 0 degrees and the angle increases by 1 degree each step to the right up to 9 degrees of tilt. The pattern continues row by row with the tilt angle increasing to the right and down until the final disc, which is in the lower left corner, is displayed at 90 degrees. Each disc has a radius of 43 pixels. Since the expected magnification results in a scale of 0.24 nanometers per pixel, this equates to a diameter of 20.64nm, which is close to the expected diameter. Each disc has a height of 20 pixels (4.8nm) and a wall thickness of 5 pixels (1.2nm). These parameters are compile-time options within the code.

The analysis image is created from the addition of the circles to a noise background. A fill value of 2348 was selected to approximate the expected value in a 12-bit image. The background noise is simulated with uniform random values ranging from 0 to 300. This matches typical noise that can be seen on other 12-bit CCD cameras. Once 12-bit images are acquired from the TEM, this can be updated to more closely match the noise of the CCD used on the TEM.

For the Maya and Blood image families, the image to be read in is set as a compile-time parameter.

6.3 Right Window

The right window shows the currently selected ROI of the entire image. This image is shown un-decimated. The cursor readout and ROI center can be changed by pressing the left mouse button. The right mouse button provides access to the 11 menu options.

- Quit – exits the program. The MS-DOS window may need to receive a <CR> to close.
- Reset Images – causes the images to be reset to the initial state. This is used in case processing has changed images and it is desired to restore them.
- Toggle show Max Point – causes a red crosshair to be displayed at the location with the maximum value.
- Process ROI w/ CORRELATION – causes the current base image to be processed with true correlation but only in the selected ROI.
- Process ROI w/ FFT CORRELATION – causes the current base image to be processed with a correlation via multiplication of FFTs followed by an inverse FFT but only in the selected ROI.
- Process Combined Image w/ CORRELATION – causes the decimated version of the current base image to be processed with true correlation.
- Process Entire Image w/ CORRELATION – causes the entire current base image to be processed with true correlation. (Note that this can take a long time to complete!)
- Process Entire Image w/ FFT CORRELATION – causes the entire current base image to be processed with a correlation via multiplication of FFTs followed by an inverse FFT.
- Process Combined Image w/ Template Series and CORRELATION – causes the decimated version of the current base image to be processed with true correlation against a series of templates. The ranges of these templates are compile-time options.
- Process Entire Image w/ Template Series and FFT CORRELATION – causes the current base image to be processed with a correlation via multiplication of FFTs followed by an inverse FFT against a series of templates. The ranges of these templates are compile-time options.
- Process ROI-centered 1Kx1K of Image w/ FFT CORRELATION – causes a 1Kx1Kpixel region of the current base image to be zero padded to 2Kx2K and processed with a correlation via multiplication of FFTs followed by an inverse FFT.